Optimization and universality of Brownian search in a basic model of quenched heterogeneous media

Aljaž Godec[1,2,*] and Ralf Metzler[1,3,†]

[1]*Institute of Physics & Astronomy, University of Potsdam, 14776 Potsdam-Golm, Germany*
[2]*National Institute of Chemistry, 1000 Ljubljana, Slovenia*
[3]*Department of Physics, Tampere University of Technology, 33101 Tampere, Finland*

The kinetics of a variety of transport-controlled processes can be reduced to the problem of determining the mean time needed to arrive at a given location for the first time, the so-called mean first-passage time (MFPT) problem. The occurrence of occasional large jumps or intermittent patterns combining various types of motion are known to outperform the standard random walk with respect to the MFPT, by reducing oversampling of space. Here we show that a regular but spatially heterogeneous random walk can significantly and universally enhance the search in any spatial dimension. In a generic minimal model we consider a spherically symmetric system comprising two concentric regions with piecewise constant diffusivity. The MFPT is analyzed under the constraint of conserved average dynamics, that is, the spatially averaged diffusivity is kept constant. Our analytical calculations and extensive numerical simulations demonstrate the existence of an optimal heterogeneity minimizing the MFPT to the target. We prove that the MFPT for a random walk is completely dominated by what we term direct trajectories towards the target and reveal a remarkable universality of the spatially heterogeneous search with respect to target size and system dimensionality. In contrast to intermittent strategies, which are most profitable in low spatial dimensions, the spatially inhomogeneous search performs best in higher dimensions. Discussing our results alongside recent experiments on single-particle tracking in living cells, we argue that the observed spatial heterogeneity may be beneficial for cellular signaling processes.

I. INTRODUCTION

Random search processes are ubiquitous in nature [1–17], ranging from the diffusive motion of regulatory molecules searching for their targets in living biological cells [5,8,18–25] and bacteria and animals searching for food by active motion [2,8] all the way to the spreading of epidemics and pandemics [3,4] and computer algorithms in high-dimensional optimization problems [26]. The fact that the search strategy in these processes is to a large extent random reflects the incapability of the searcher to keep track of past explorations at least over more than a certain period [5]. Over the years several different search strategies have been studied in the literature, including Brownian motion [8,18,27,28], spatiotemporally decoupled Lévy flights (LFs) [29–34], and coupled Lévy walks (LWs) [35–46] in which the searcher undergoes large relocations with a heavy-tailed length distribution either instantaneously (LFs) or with constant speed (LWs), as well as intermittent search patterns, in which the searcher combines different types of motion [5], for instance, three-dimensional and one-dimensional diffusion [18–25,47,48], three-dimensional and two-dimensional diffusion [49,50], or diffusive and ballistic motion [5,8,51–57].

The efficiency of the search strategy is conventionally quantified via the mean first-passage time (MFPT) defined as the average time a random searcher needs to arrive at the target for the first time [5,27,28,58,59]. The physical principle underlying an improved search efficiency is an optimized balance between the sampling of space on a scale much larger than the target and on a scale similar to or smaller than the target [5]. More specifically, periods of less-compact exploration, for instance, diffusion in higher dimensions, Lévy flights, or ballistic motion, aid towards bringing the searcher faster into the vicinity of the target. Concurrently, a searcher in such a less-compact search mode may thereby easily overshoot the target [32,33]. In contrast, compact exploration of space (for instance, diffusion in one dimension) is superior when it comes to hitting the target from close proximity, but performs worse when it comes to the motion on larger scales taking the searcher from its starting position into the target's vicinity: Typically frequent returns occur to the same location, a phenomenon referred to as oversampling. Mathematically, this is connected to the recurrent nature of such compact random processes. The idea behind search optimization is to find an optimal balance of both more- and less-compact search modes in the given physical setting [5]. For instance, in the so-called facilitated diffusion model for the target search of regulatory proteins on DNA [19–23], the average duration of noncompact three-dimensional free diffusion is balanced by an optimal compact one-dimensional sliding regime along the DNA molecule. In an intermittent search [5,8,51] persistent ballistic excursions are balanced by compact Brownian phases. This optimization principle intuitively works better in lower dimensions, where a searcher performing a standard random walk oversamples the space. Hence, the typically considered optimized strategies have the largest gain in low dimensions.

In a variety of experimental situations the motion of a searcher is characterized by the same search strategy but is not translationally invariant. A typical example is a system in which the searcher performs a standard random walk but with a spatially varying rate of making its steps. This type of motion is actually abundant in biological cells, where

---

*agodec@uni-potsdam.de
†rmetzler@uni-potsdam.de

experiments revealed a distinct spatial heterogeneity of the protein diffusivity [60–62]. Several aspects of such diffusion in heterogeneous media have already been addressed [27,63–67], but the generic first-passage time properties remain elusive, in particular, for quenched environments.

Here was ask the question whether spatial heterogeneity is generically detrimental for the efficiency of a random search process or whether it could even be beneficial. Could it even be true that proteins find their targets on the genome in the nucleus faster because their diffusivity landscape in the cell is heterogeneous? On the basis of exact results for the MFPT in one, two, and three dimensions in a closed domain under various settings we show here that a spatially heterogeneous search can indeed significantly enhance the rate of arrival at the target. We explain the physical basis of this acceleration compared to a homogeneous search process and quantify an *optimal heterogeneity*, which minimizes the MFPT to the target. Furthermore, we show that heterogeneity can be generically beneficial in a random system and is thus a robust means of enhancing the search kinetics. The optimal heterogeneous search rests on the remarkable observation that the MFPT is completely dominated by those *direct* trajectories heading directly towards the target. We prove that the MFPT for the heterogeneous system can be exactly described with the results of a standard random walk. We compare our theoretical findings to recent experiments on single-particle tracking in living cells, which are indeed in line with the requirements for enhanced search.

The paper is organized as follows. Section II introduces our minimal model for heterogeneous search processes. In Sec. III we briefly summarize our main general results, which hold irrespective of the dimension ($d = 1, 2,$ or 3). Section IV is devoted to the analysis of the most general situation with a specific starting point and position of the interface. In Sec. V we focus on the global MFPT, that is, the MFPT averaged over the initial position. In Sec. VI we analyze a system with a random position of the interface and optimize the MFPT averaged over the interface position. In Sec. VII we address the global MFPT in systems with a random position of the interface. Throughout we discuss our results in a biophysical context motivated by recent experimental findings. We conclude in Sec. VIII by discussing the implications of our results for more general spatially heterogeneous systems.

II. MINIMAL MODEL FOR SPATIALLY HETEROGENEOUS RANDOM SEARCH

We focus on the simplest scenario of a spatially heterogeneous system. Even for this minimal model the analysis turns out to be challenging and our exact results reveal a rich behavior with several *a priori* surprising features. We consider a spherically symmetric system in dimensions $d = 1, 2,$ and 3 with a perfectly absorbing target of radius a located in the center (Fig. 1). The outer boundary at radius R is taken to be perfectly reflecting. The system consists of two domains with uniform diffusivities denoted by D_1 and D_2 in the interior and exterior domains, respectively. The interface between these domains is located at r_I. The microscopic picture we are considering corresponds to the kinetic interpretation of the Langevin or corresponding Fokker-Planck equations. In
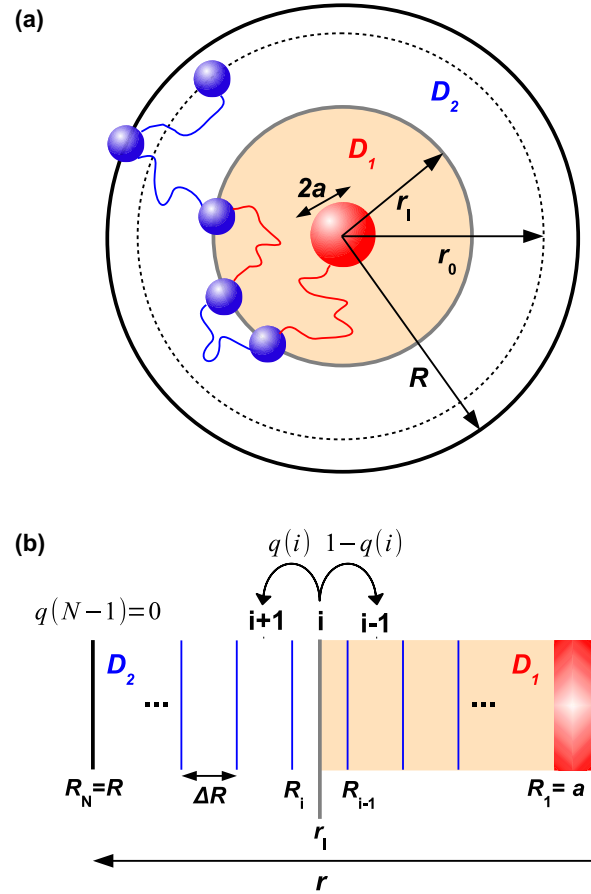

FIG. 1. (Color online) Schematic of the model system: (a) A spherical target with radius a is placed in the center of a spherical domain of radius R. The free space between the radii a and R is divided into two regions denoted by subscripts. The inner region is bounded by a shell at radius r_I. The outer region ranges from r_I to the reflective boundary at R. Initially, the particle's starting position is uniformly distributed over the surface of the sphere with radius r_0. (b) Microscopic picture of the problem starting from a discrete random walk between spherical shells. The hopping rates are assumed to obey detailed balance and the interface position is chosen to be placed symmetrically between two concentric spherical surfaces.

particular we assume that the dynamics obey the fluctuation-dissipation relation and in the steady state agree with the results of equilibrium statistical mechanics [68].

In the biological context we consider that the system is in contact with a heat bath at constant and uniform temperature T. The signaling proteins diffuse in a medium comprising water and numerous other particles, such as other biomacro-molecules or cellular organelles. The remaining particles, which we briefly call crowders, are not uniformly distributed across the cell: Their identity and relative concentrations differ within the nucleus and the cytoplasm and can also show variations across the cytoplasm. The proteins hence experience a spatially varying friction $\Gamma(\mathbf{r})$, which originates from spatial variations in the long-range hydrodynamic coupling to the motion of the crowders, which is in turn mediated by the solvent [69,70]. The proteins thus move under the influence of a position-dependent diffusion coefficient $D(\mathbf{r}) = 2k_B T \Gamma(\mathbf{r})$

and a fluctuation-induced thermal drift $\boldsymbol{F}(\boldsymbol{r}) \sim k_B T \boldsymbol{\nabla} \Gamma(\boldsymbol{r})$ (see [71] for details). The vital role of such hydrodynamic interactions in the cell cytoplasm was demonstrated in [72].

Because of the spherical symmetry of the problem we can reduce the analysis to the radial coordinate alone. That is, we only trace the projection of the motion of the searcher onto the radial coordinate and therefore start with a discrete space-time nearest-neighbor random walk in between thin concentric spherical shells of equal width $\Delta R = R_{i+1} - R_i$ as depicted in Fig. 1. The shell i denotes the region between surfaces with radii R_{i-1} and R_i. We assume that the hopping rates between shells $\Pi(i \rightarrow j)$ obey detailed balance

$$p(i)\Pi(i \rightarrow i+1) = p(i+1)\Pi(i+1 \rightarrow i). \quad (1a)$$

Here $p(i)$ denotes the probability distribution of finding the particle in shell i. The hopping rates Π are given as the product of the intrinsic rate $2D(i)/\Delta R^2$ and $q(i)$, the probability to jump from shell i to shell $i+1$ [and $1-q(i)$ for jumps in the other direction],

$$\Pi(i \rightarrow i+1) = \frac{2D(i)}{\Delta R^2} q(i). \quad (1b)$$

Here $D(i)$ is the arithmetic mean of the diffusivity in shell i. The rate $q(i)$ can be derived as follows. A random walker located in shell i at time t can either move to shell $i+1$ with probability $q(i)$ or to shell $i-1$ with probability $1-q(i)$. Due to the isotropic motion of the random walker, these probabilities are proportional to the respective surface areas of the bounding d-dimensional spherical surfaces at R_{i-1} and R_i, that is, $q(i) \sim R_i^{d-1}$ and $1-q(i) \sim R_{i-1}^{d-1}$. The proportionality constant is readily obtained from the normalization condition leading to

$$q(i) = \frac{R_i^{d-1}}{R_i^{d-1} + R_{i-1}^{d-1}} \quad (1c)$$

and thus $1-q(i) = R_{i-1}^{d-1}/(R_i^{d-1} + R_{i-1}^{d-1})$. Therefore, while the random walker moves in all directions (radial, azimuthal, or polar) we can project its motion on the radial coordinate only. We assume that the interface is located between two concentric shells leading to a continuous steady-state probability density profile. The searcher starts at $t=0$ uniformly distributed over the surface of a d sphere with radius r_0, as sketched in Fig. 1(a).

In our analytical calculations we model the system in terms of the probability density function $p(r,t|r_0)$ to find the particle at radius r at time t after starting from radius r_0 at $t=0$. Here $p(r,t|r_0)$ obeys the radial diffusion equation

$$\frac{\partial p(r,t|r_0)}{\partial t} = \frac{1}{r^{d-1}} \frac{\partial}{\partial r} \left(D(r) r^{d-1} \frac{\partial}{\partial r} \right) p(r,t|r_0) \quad (2a)$$

with a position-dependent diffusivity $D(r)$. Here we consider the simplest version of a piecewise constant diffusivity

$$D(r) = \begin{cases} D_1, & a < r \leqslant r_I \\ D_2, & r_I < r \leqslant R. \end{cases} \quad (2b)$$

We assume that the target surface at radius a is perfectly absorbing,

$$p(a,t|r_0) = 0, \quad (2c)$$

to determine the first-passage behavior. At the outer radius R we use the reflecting boundary condition

$$\left. \frac{\partial p(r,t|r_0)}{\partial r} \right|_{r=R} = 0. \quad (2d)$$

These boundary conditions are complemented by joining conditions at r_I by requiring the continuity of the probability density and the flux, which follow from our microscopic picture.

To quantify our model system we introduce the ratio

$$\varphi = \frac{D_1}{D_2} \quad (3a)$$

of the inner and outer diffusivities. Moreover, we demand that the spatially averaged diffusivity

$$\overline{D} = \frac{d}{R^d - a^d} \int_a^R r^{d-1} D(r) dr \quad (3b)$$

remains constant for varying D_1 and D_2. Without such a constraint the problem of finding an optimal φ, which minimizes the MFPT, is ill posed and has a trivial solution $\varphi = \infty$. More importantly, we want to compare the search efficiency as a function of the degree of heterogeneity, where the overall intensity of the dynamics is conserved. Returning to our microscopic picture of a signaling protein searching for its target in the nucleus, the heterogeneous diffusivity is due to spatial variations in the long-range hydrodynamic coupling to the motion of the crowders. Their identity and relative concentration in the cell vary in space, but the effect is mediated by thermal fluctuations in the solvent at a constant temperature. The constraint in Eq. (3b) then corresponds to a redistribution of the crowders at constant temperature, cell volume, and numbers of the various crowders, which would not affect the spatially averaged diffusivity.

Under the constraint (3b) of constant spatially averaged diffusivity we obtain for any given φ and r_I that

$$D_1 = \frac{\varphi \overline{D}}{(\varphi - 1)\chi(r_I) + 1}, \quad D_2 = \frac{\overline{D}}{(\varphi - 1)\chi(r_I) + 1}, \quad (4a)$$

where we introduced the hypervolume ratio

$$\chi(r_I) = \frac{r_I^d - a^d}{R^d - a^d} \quad (4b)$$

of the inner versus the entire domain excluding the target volume. To solve Eq. (2a) we take a Laplace transform in time and the obtained Bessel-type equation is solved exactly as shown in Sec. IV. The MFPT $\mathbf{T}(r_0)$ for the particle to reach the target surface at $r=a$ is obtained from the Laplace transformed flux into the target

$$\widetilde{j}(r_0,s) = \Omega_d D_1 a^{d-1} \left. \frac{\partial \widetilde{P}(r,r_0,s)}{\partial r} \right|_{r=a} \quad (5a)$$

via the relation

$$\mathbf{T}(r_0) = -\left. \frac{\partial \widetilde{j}_a(r_0,s)}{\partial s} \right|_{s=0}. \quad (5b)$$

The angular prefactor $\Omega_d = 1$ for $d=1$, $\Omega_d = 2\pi$ for $d=2$, and $\Omega_d = 4\pi$ for $d=3$. We treat the degree of heterogeneity φ as an adjustable parameter at a fixed value

of r_I and seek an optimal value minimizing the MFPT. The optimal heterogeneity, which we denote by an asterisk, is thus obtained by extremizing $\mathbf{T}_a(r_0)$ with respect to φ.

III. SUMMARY OF THE MAIN RESULTS

Since R in combination with the diffusivity $\overline{D}$ sets the absolute time scale, we can express, without loss of generality, time in units of $R^2/\overline{D}$, set $\overline{D} = 1$, and focus on the problem in a unit sphere. We introduce dimensionless spatial units $x_a = a/R$, $x_I = r_I/R$, and $x_0 = r_0/R$. For the sake of completeness, we retain the explicit R and $\overline{D}$ dependence in the prefactors.

Our first main result represents the fact that the MFPT to the target in the inhomogeneous system in dimensions $d = 1$, 2, and 3 can be expressed exactly in terms of the corresponding MFPT $\mathbf{T}^0(x_0; D_i)$ in a *homogeneous* system with diffusivity D_i, with $i = 1$ or 2. Remarkably, the MFPT is thus exactly equal to

$$\mathbf{T}(x_0) = \begin{cases} \mathbf{T}^0(x_0; D_1), & x_0 \leqslant x_I \\ \mathbf{T}^0(x_I; D_1) + \mathbf{T}^0_{x_I}(x_0; D_2), & x_0 > x_I. \end{cases} \quad (6)$$

In the second line the argument x_I stands for the release of the particle at the interface and the index x_I of the last term is used to indicate that this term measures the first passage to the interface at x_I. That is, in this case when the particle starts in the inner region with diffusivity D_1, Eq. (6) reveals that the MFPT of the heterogeneous system is equal to that of a homogeneous system with diffusivity D_1 everywhere and is independent of the position of the interface. Conversely, if the searcher starts in the exterior region with diffusivity D_2 the MFPT contains two contributions: (i) the MFPT from r_0 to r_I in a homogeneous system with diffusivity D_2 and (ii) the MFPT from r_I to a in a homogeneous system with diffusivity D_1, as shown schematically in Fig. 2. Equation (6) is exact and independent of the choice for $D_{1,2}$ and thus holds for an arbitrary set of diffusivities and even if $D_1 = D_2$. In other words, it is not a consequence of a conserved $\overline{D}$. Note that if one starts from different mathematical assumptions for the inclusion of inhomogeneous step frequencies, a result different from Eq. (6) emerges [73].

The additivity principle of the individual MFPTs in Eq. (6) is only possible if the excursions of the searcher in the directions away from the target are statistically insignificant. We would expect that some trajectories starting in the inner region will carry the searcher into the outer region with diffusivity D_2 before the searcher eventually crosses the interface and reaches the target by moving through the inner region with diffusivity D_1. Such trajectories will obviously be different in the heterogeneous system in comparison to a homogeneous system with diffusivity D_1 everywhere. This
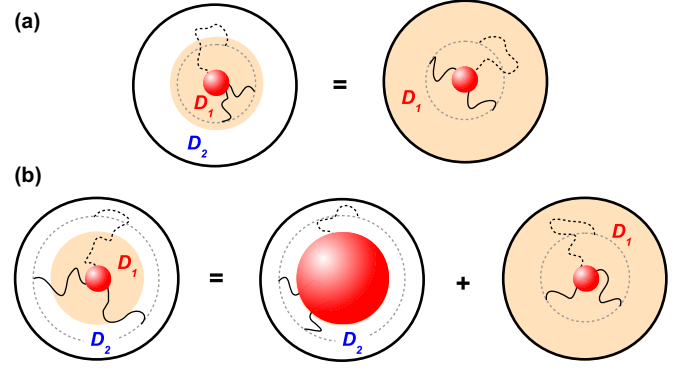

FIG. 2. (Color online) Schematic of the equivalence of MFPTs in inhomogeneous and homogeneous systems in the case of (a) a searcher starting in the inner region and (b) a searcher starting in the outer region. The radius x_1 of the initial particle position is shown by the thin dashed circle. We show direct trajectories as solid lines. Each panel also contains an indirect trajectory (dashed line) that leads the particle into the outer region of the system. As our analysis shows direct trajectories dominate the MFPT.

appears to contradict the complete independence of D_2 of the MFPT in Eq. (6) for trajectories with $x_0 \leqslant x_I$. This observation can be explained by the dominance of *direct trajectories*, whose occupation fraction outside the starting radius is statistically insignificant: The MFPT for a standard random walk in dimensions $d = 1$, 2, and 3 is completely dominated by direct trajectories. As such, the MFPT is really a measure for the efficiency of the direct trajectories. We note that if the walker starts in the outer region ($x_0 > x_I$), as intuitively expected, the MFPT diverges with vanishing D_2.

Our second main result demonstrates that for $x_0 > x_I$ a finite optimal heterogeneity exists at a given interface position and is given by

$$\varphi^*(x_0) = \sqrt{\frac{1 - \chi(x_I)}{\chi(x_I)} \frac{\mathbf{T}^0(x_I; 1)}{\mathbf{T}^0_{x_I}(x_0; 1)}}. \quad (7)$$

For this value the MFPT $\mathbf{T}(x_0)$ attains a minimum. Hence, the optimal heterogeneity is completely determined by the volume fractions and the MFPT properties and hence strictly by the direct trajectories. As above, the index x_I in the MFPT $\mathbf{T}^0(x_I)$ indicates the first passage to the interface, while without this index the MFPT $\mathbf{T}^0$ quantifies the first passage to the target at x_a. The explicit results for $\varphi^*(x_0)$ are shown in Fig. 4 and are discussed in detail in Sec. IV.

Often one is interested in the MFPT averaged over an ensemble of starting positions, the global MFPT $\overline{\mathbf{T}}$. As before, it can be shown that an optimal heterogeneity exists for any interface position and is universally given by

$$\overline{\varphi}^* = \left(\frac{1 - \chi(x_I)}{\chi(x_I)} \frac{\mathbf{T}^0(x_I; 1) - \int_{x_a}^{x_I} \left[x_0^d (d/dx_0) \mathbf{T}^0(x_0; 1) \right] dx_0}{\mathbf{T}^0_{x_I}(1; 1) - \int_{x_I}^{1} \left[x_0^d (d/dx_0) \mathbf{T}^0_{x_I}(x_0; 1) \right] dx_0} \right)^{1/2}. \quad (8)$$

Similar to the general case, $\overline{\varphi}^*$ is again proportional to $[\chi(x_I)^{-1} - 1]^{1/2}$ but here the corresponding MFPTs in the second factor are reduced by a spatially averaged change of the MFPT with respect to the starting position. The optimal heterogeneity for the global MFPT is shown in Fig. 5 and discussed in detail in Sec. V.

In a setting when the interface position is random and uniformly distributed we are interested in the MFPT from a given starting position averaged over the interface position. A measurable quantity for this scenario for an ensemble of random-interface systems is the MFPT $\{\mathbf{T}_a(x_0)\}$, where the curly brackets denote an average over the interface positions x_I. Explicit results for dimensions $d = 1, 2$, and 3 are given in Sec. VI. Solving for the optimal heterogeneity, we obtain

$$\{\varphi\}^* = \left(\frac{\mathbf{T}^0(x_0) - (1 + 1/d) \int_{x_a}^{x_0} x[1 - x^d/(d+1)][(d/dx_I)\mathbf{T}^0(x_I)]dx_I}{x_a^{d+1}\mathbf{T}^0(x_0) - (1 + 1/d) \int_{x_a}^{x_0} x[x^d/(d+1) - x_a^d][(d/dx_I)\mathbf{T}_{x_I}^0(x_0)]dx_I} \right)^{1/2}. \tag{9}$$

The optimal heterogeneity for the MFPT averaged over the random interface position is shown in Fig. 6.

Finally, we compute the global MFPT averaged over the position of the interface $\{\overline{\mathbf{T}}\}$ whose explicit results are given in Sec. VI. Also here an optimal strategy can be identified as

$$\{\overline{\varphi}\}^* = \left(\frac{\overline{\mathbf{T}}^0 - \int_{x_a}^1 (1 - x_I)x_I^d\left(1 + d - x_I^d\right)/\left(1 - x_a^d\right)(d/dx_I)\mathbf{T}^0(x_I; 1)dx_I}{x_a^{d+1}\overline{\mathbf{T}}^0 - \int_{x_a}^1 x_I^d\left[x_I^d - (1+d)x_a^d\right]/\left(1 - x_a^d\right)(d/dx_I)\overline{\mathbf{T}}_{x_I}^0 dx_I} \right)^{1/2}. \tag{10}$$

The optimal heterogeneity for the global MFPT averaged over the random interface position is shown in Fig. 7.

Equation (6) represents a rigorous proof that direct trajectories dominate the MFPT for Brownian motion. In addition, the heterogeneity does not affect the fraction of direct versus indirect trajectories but only their respective durations. Due to the fact that indirect trajectories are statistically insignificant, we can in principle make them arbitrarily slow if we start in the inner region. However, as we let the inner diffusivity go to infinity (and hence the outer one to zero) we are simultaneously slowing down the arrivals to the interface if starting from the outer region. The following is the physical principle underlying the acceleration of search kinetics: The optimal heterogeneity

corresponds to an improved balance between the MFPT to reach the interface and the one to reach the target from the interface.

IV. MEAN FIRST-PASSAGE TIME FOR FIXED INITIAL AND INTERFACE POSITIONS

Here we present the mathematical derivation and the explicit results for the situation with a specific initial condition r_0 and interface position r_I. Equation (2a) is solved by Laplace transformation and the resulting Green's function with the boundary conditions (2c) and (2d) reads

$$\widetilde{P}(r,s|r_0) = \frac{(rr_0)^\nu}{\Omega_d D_1} \left[\mathcal{C}_\nu(S_1 r, S_1 a) \middle/ \left(\frac{\mathcal{D}_\nu(S_1 a, S_1 r_I)}{\mathcal{C}_{\nu-1}(S_2 r_I, S_2 R)} + \frac{1}{\sqrt{\varphi}} \frac{\mathcal{C}_\nu(S_1 a, S_1 r_I)}{\mathcal{D}_\nu(S_2 r_I, S_2 R)} \right) \right]$$

$$\times \begin{cases} \dfrac{\mathcal{D}_\nu(S_1 r_0, S_1 r_I)}{\mathcal{C}_{\nu-1}(S_2 r_I, S_2 R)} + \dfrac{1}{\sqrt{\varphi}} \dfrac{\mathcal{C}_\nu(S_1 r_0, S_1 r_I)}{\mathcal{D}_\nu(S_2 r_I, S_2 R)}, & a < r_0 \leqslant r_I \\[3mm] \dfrac{\mathcal{D}_\nu(S_2 r_0, S_2 R)}{r_I S_1 \mathcal{D}_\nu(S_2 r_I, S_2 R)\mathcal{C}_{\nu-1}(S_2 r_I, S_2 R)}, & r_I < r_0 \leqslant R, \end{cases} \tag{11a}$$

where we introduced the abbreviation $S_{1,2} = \sqrt{s/D_{1,2}}$ and the auxiliary functions

$$\begin{aligned} \mathcal{D}_\nu(z_1, z_2) &= I_\nu(z_1)K_{\nu-1}(z_2) + K_\nu(z_1)I_{\nu-1}(z_2), \\ \mathcal{C}_\nu(z_1, z_2) &= I_\nu(z_1)K_\nu(z_2) - I_\nu(z_2)K_\nu(z_1). \end{aligned} \tag{11b}$$

Here the $I_\nu(z)$ and $K_\nu(z)$ denote the modified Bessel functions of order $\nu = 1 - d/2$ of the first and second kinds, respectively. The Laplace transformed first-passage time density is obtained from the flux (5a) into the target and the MFPT then follows from relation (5b). In the case of $d = 1$ the target

size only enters the problem by determining the width of the interval. Using $\mathcal{D}_\nu(z,z) = 1/z$, it can be shown that Eq. (11a) reduces to the ordinary expression for regular diffusion given in Ref. [27] for $r_I = R$ and $\varphi = 1$.

The MFPT can be written exactly in terms of the expressions for a homogeneous diffusion process in Eq. (6) (compare Refs. [27,58]) and we obtain

$$_1\mathbf{T}^0(x_0; \overline{D}) = \frac{R^2}{2\overline{D}}\left[2(x_0 - x_a) + x_a^2 - x_0^2\right], \tag{12a}$$
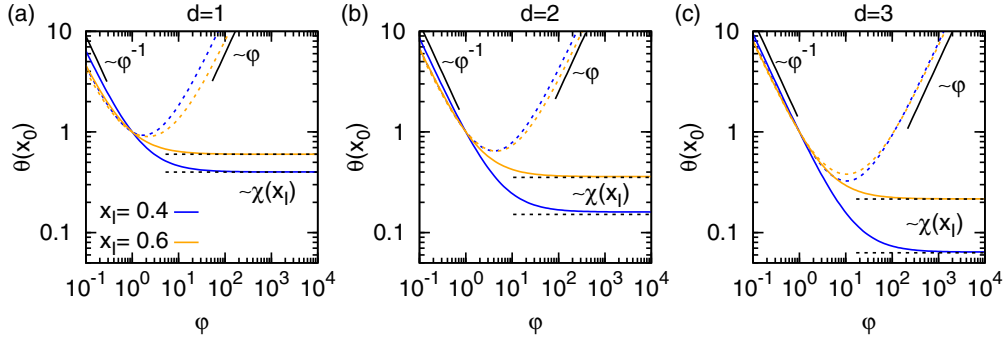
FIG. 3. (Color online) Ratio $\theta(x_0) = \mathbf{T}(x_0)/\mathbf{T}^0(x_0)$ as a function of $\varphi = D_1/D_2$ in dimensions (a) $d = 1$, (b) $d = 2$, and (c) $d = 3$ for initial radii $x_0 = 0.3$ (dashed lines) and $x_0 = 0.8$ (solid lines), respectively. In (b) and (c) we plot the results for a target size $x_a = 0.1$. The solid black lines denote the $\simeq 1/\varphi$ and $\simeq \varphi$ scalings, respectively, and the dashed black line corresponds to $\simeq \chi(x_{\mathrm{I}})$.

$$_2\mathbf{T}^0(x_0; \overline{D}) = \frac{R^2}{4\overline{D}}\left[2\ln\left(\frac{x_0}{x_a}\right) + x_a^2 - x_0^2\right], \quad (12b)$$

$$_3\mathbf{T}^0(x_0; \overline{D}) = \frac{R^2}{6\overline{D}}\left[2\frac{x_0 - x_a}{x_0 x_a} + x_a^2 - x_0^2\right]. \quad (12c)$$

Here the left index denotes the dimensionality of the system. Note that the parameter R in Eqs. (6) and (12) only sets the corresponding time scale via $\tau_n = R^2/2d\overline{D}$, but otherwise completely factors out of the MFPT problem. In other words, the problem is fully described by the search in a hypersphere of unit radius, where time is measured in units of τ_n. In an infinite system such a time scale ceases to exist and the corresponding MFPT diverges. Our results show excellent agreement with numerical simulations, as demonstrated in the Appendix. Plugging the above expressions (12) into Eq. (6), we can compare the search efficiency with respect to a homogeneous random walk by introducing the dimensionless ratio

$$\theta(x_0) = \frac{\mathbf{T}(x_0)}{\mathbf{T}^0(x_0)}. \quad (13)$$

The corresponding results for dimensions $d = 1$, 2, and 3 are shown in Fig. 3. As a nonzero x_a in $d = 1$ only rescales the size of the domain $R \to R(1 - x_a)$, we will in the following set $x_a = 0$ in $d = 1$.

The qualitative behavior of the MFPT with respect to φ, that is, the degree of the heterogeneity, depends on the starting position relative to the interface. If the initial position lies in the inner region $\theta(x_0)$ decays monotonically and saturates at a finite asymptotic value $\theta(x_0) \to \chi(x_{\mathrm{I}})$. Hence, in this case an optimal strategy does not exists and the best search performance is achieved for large diffusivities in the inner region. The lower bound on $\theta(x_0)$ is set by the volume fraction of the inner region, which sets a bound on the ratio $D_1/\overline{D}$. This result is yet another manifestation of the fact that the MFPT is completely dominated by direct trajectories.

Conversely, if the searcher starts in the outer region an optimal strategy exists. To understand the existence and meaning of the optimal heterogeneity we perform a power-series expansion of $\theta(x_0)$. We find the scaling $\theta(x_0) \simeq 1/\varphi$ as $\varphi \to 0$, which is due to the fact that in this regime $D_1 \simeq \varphi$,

which dominates the MFPT in this regime. In the other limit as $\varphi \to \infty$ we find $\theta(x_0) \simeq \varphi$ because here $D_2 \simeq 1/\varphi$ and the rate-determining step is the arrival at the interface. We can understand the optimal heterogeneity as a beneficial balance between the rate of arriving at the interface from the starting position and the rate to find the target if starting from the interface.

In contrast, too large values of φ prolong the time to reach the interface and cannot be compensated by a faster arrival from the interface towards the target. The optimal heterogeneity as a function of the starting position is shown in Figs. 4(a)–4(c) and reveals the divergence as $x_0 \to x_{\mathrm{I}}$: This point corresponds to the disappearance of an optimal strategy. As x_0 gradually approaches unity, φ^* continuously decreases towards a plateau, which suggests that reaching the target from the interface becomes the rate-determining step. Moreover, φ^* decreases with increasing target size, because the inner region becomes smaller and thus allows a larger D_2 in the optimal scenario. The overall gain of an optimal search with respect to a standard random walk is shown in Figs. 4(d)–4(f). Only in the domain $x_0 > x_{\mathrm{I}}$ an optimal heterogeneity exists, therefore we omitted the region $x_0 < x_{\mathrm{I}}$. As mentioned before, we observe the monotonic convergence $\theta(x_0) \to \chi(x_{\mathrm{I}})$ from above as $\varphi \to \infty$ and hence the heterogeneous search always outperforms the standard Brownian search for $\varphi > 1$. The highest gain is therefore set by the volume fraction of the inner region, which becomes arbitrarily small as $x_{\mathrm{I}} \to x_a$. For $x_0 > x_{\mathrm{I}}$ we find that the gain is largest for starting positions near the interface and when the interface is not too close to the outer boundary, where the system essentially approaches the homogeneous limit. The variations are larger in higher dimensions, which is, of course, connected with the pronounced spatial oversampling in lower d.

Different from conventional strategies, intermittent or Lévy-stable processes, which affect the compactness of exploring space, a heterogeneous search is more profitable in higher dimensions [see Figs. 4(d)–4(f)]. Because heterogeneity acts by enhancing and retarding the local dynamics and does not affect spatial oversampling, it is intuitive that it performs better for noncompact exploration of space. Both the existence and the gain of an optimally heterogeneous search are thus a direct consequence of direct trajectories dominating the MFPT.
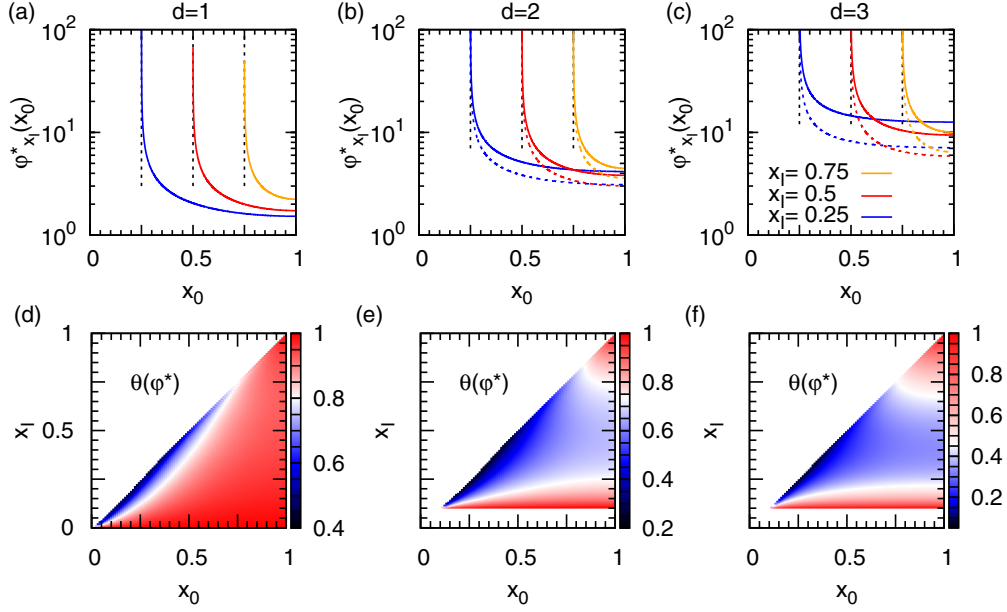
FIG. 4. (Color online) Optimal heterogeneity as a function of the starting position x_0 for three interface positions $x_I = 0.25$ (blue), $x_I = 0.5$ (red), and $x_I = 0.75$ (orange) in dimensions (a) $d = 1$, (b) $d = 2$, and (c) $d = 3$. The target sizes in (b) and (c) are $x_a = 0.1$ (solid lines) and $x_a = 0.2$ (dashed lines). Also shown is the ratio $\theta(x_0) = \mathbf{T}(x_0)/\mathbf{T}^0(x_0)$ for the optimal heterogeneity φ^* in dimensions (d) $d = 1$, (e) $d = 2$, and (f) $d = 3$. In (e) and (f) the target size is $x_a = 0.1$.

V. GLOBAL MEAN FIRST-PASSAGE TIME FOR FIXED INTERFACE POSITION

The global MFPT is obtained by direct averaging of Eq. (6) over the initial position x_0,

$$\overline{\mathbf{T}} = \frac{d}{1 - x_a^d} \int_{x_a}^1 x_0^{d-1} \mathbf{T}(x_0) dx_0. \tag{14}$$

The exact expressions for the global MFPT in the various dimensions read

$$_1\overline{\mathbf{T}} = \frac{R^2[(1 - 1/\varphi)x_I + 1/\varphi]}{\overline{D}} \left[\frac{\varphi}{3} + x_I(1 - \varphi) - x_I^2(1 - \varphi) + \frac{x_I^3(1 - \varphi)}{3} \right], \tag{15a}$$

$$_2\overline{\mathbf{T}} = \frac{R^2[(1 - 1/\varphi)x_I^2 + 1/\varphi - x_a^2]}{4\overline{D}(1 - x_a^2)^2} \left[2(1 - \varphi)\ln(x_I) - 2\ln(x_a) - (x_I^2 - x_a^2)\left(2 - \frac{x_I^2 + x_a^2}{2}\right) - \varphi\left(\frac{3}{2} - 2x_I + \frac{x_I^4}{2}\right) \right], \tag{15b}$$

$$_3\overline{\mathbf{T}} = \frac{R^2[(1 - 1/\varphi)x_I^3 + 1/\varphi - x_a^3]}{6\overline{D}(1 - x_a^3)^2} \left[\frac{2}{x_a} + \frac{2(\varphi - 1)}{x_I} + 2x_I^2(\varphi - 1)\left(1 - \frac{x_I^3}{5}\right) - \frac{9\varphi}{5} + 2x_a^2\left(1 - \frac{x_a^3}{5}\right) \right]. \tag{15c}$$

These are to be compared with their homogeneous counterparts

$$_1\overline{\mathbf{T}}^0 = \frac{R^2}{3\overline{D}}, \tag{16a}$$

$$_2\overline{\mathbf{T}}^0 = \frac{R^2}{4\overline{D}(1 - x_a^2)^2} \left[-\frac{3}{2} + 2x_a^2 - \frac{x_a^4}{2} - 2\ln(x_a) \right], \tag{16b}$$

$$_3\overline{\mathbf{T}}^0 = \frac{R^2}{3\overline{D}(1 - x_a^3)^2} \left[1 - \frac{9x_a}{5} + x_a^3\left(1 - \frac{x_a^3}{5}\right) \right] \tag{16c}$$

in $d = 1$, 2, and 3, respectively. As before, we introduce the dimensionless enhancement ratio

$$\overline{\theta} = \frac{\overline{\mathbf{T}}}{\overline{\mathbf{T}}^0}. \tag{17}$$

The results are shown in Fig. 5. In this case we are effectively considering a weighted average of the results presented in Sec. IV. Noticing that most of the volume of a d-sphere is increasingly concentrated near the surface for growing
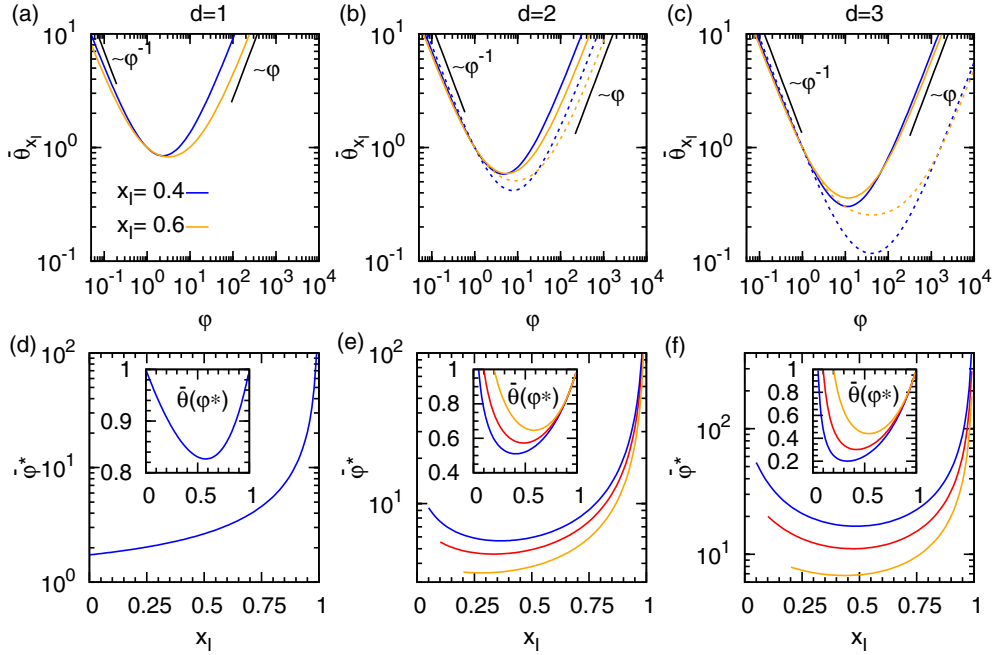
FIG. 5. (Color online) Ratio $\bar{\theta} = \overline{\mathbf{T}}/\overline{\mathbf{T}}^0$ as a function of $\varphi = D_1/D_2$ for different dimensions and interface positions $x_\mathrm{I} = 0.4$ (blue) and $x_\mathrm{I} = 0.6$ (orange). The target sizes in (b) and (c) are $x_a = 0.1$ (solid lines) and $x_a = 0.2$ (dashed lines). (d)–(f) Optimal heterogeneity for different dimensions as a function of the interface position x_I. In (e) and (f) the target sizes are $x_a = 0.05$ (blue), $x_a = 0.1$ (red), and $x_a = 0.2$ (orange). The insets in (d)–(f) show $\bar{\theta}$ for the optimal heterogeneity $\overline{\varphi}^*$.

dimensions, we anticipate that the results will be more prominently influenced by the features of trajectories starting farther away from the target. An interesting question will therefore be whether an optimal heterogeneity exists for all interface positions and dimensions. An expansion of $\overline{\mathbf{T}}$ in a power series of φ reveals that $\bar{\theta} \simeq 1/\varphi$ as $\varphi \to 0$ and $\bar{\theta} \simeq \varphi$ as $\varphi \to \infty$ for all positions of the interface [see Figs. 5(a)–5(c)]. Thus, an optimal heterogeneity always exists for all d. From Figs. 5(a)–5(c) we observe that the dependence of the relative gain compared to $\bar{\theta}$ on the interface position in the limit $\varphi \to 0$ is very weak in all dimensions as long as it is not too close to the external boundary. In the case of large φ somewhat larger

variations are observed for dimensions $d = 1$ and 2. In $d = 3$ the dependence on the interface position is largest near the optimal value for $\overline{\varphi}$ but very weak elsewhere. Hence, a control of the target location dynamics by adjusting x_I is only efficient near the optimal point $\overline{\varphi} = \overline{\varphi}^*$. This is observed from the respective scalings $\bar{\theta} \simeq 1/\varphi$ and $\bar{\theta} \simeq \varphi$ as $\varphi \to 0$ and $\varphi \to \infty$ as explained in Sec. IV. Overall, the gain with respect to the homogeneous random walk is larger for higher dimensions, which has the same origin as in the general case discussed above, however here the additional effect of averaging over the initial position enters. The optimal heterogeneity has the exact results

$$_1\overline{\varphi}^* = \frac{\sqrt{3(1 - x_\mathrm{I}) + x_\mathrm{I}^2}}{1 - x_\mathrm{I}},$$ (18a)

$$_2\overline{\varphi}^* = \left(\frac{(1 - x_\mathrm{I}^2)\left\{ -4 + x_\mathrm{I}^2 + x_a^2 + \left[4/(x_\mathrm{I}^2 - x_a^2) \right] \ln(x_\mathrm{I}/x_a) \right\}}{-4\ln(x_\mathrm{I}) - 3 + 4x_\mathrm{I}^2 - x_\mathrm{I}^4} \right)^{1/2},$$ (18b)

$$_3\overline{\varphi}^* = \left((1 - x_\mathrm{I}^3) \frac{5\left[(x_\mathrm{I}/x_a)(1 + x_a^3) - (1 + x_\mathrm{I}^3) \right] + x_\mathrm{I}(x_\mathrm{I}^5 - x_a^5)}{(1 - x_\mathrm{I})^3 \{ 5 + x_\mathrm{I}[6 + x_\mathrm{I}(3 + x_\mathrm{I})] \}} \right)^{1/2}.$$ (18c)

The behavior of Eqs. (18) is shown in Figs. 5(e) and 5(f). In higher dimensions the optimal heterogeneity shows a non-monotonic behavior with respect to the interface position and increases upon approaching the target or the outer boundary. Simultaneously, the overall dependence of the global MFPT on φ vanishes in these limits [see the insets of Figs. 5(e) and 5(f)], corresponding to the situation when the system is no longer heterogeneous. These results can be rationalized by the fact that in the limit $x_\mathrm{I} \to x_a$ the ratio $\chi(x_\mathrm{I})$ becomes negligible and hence a higher D_1 is allowed without slowing down the dynamics of reaching the interface from the external region. Conversely, as $x_\mathrm{I} \to 1$ also $\chi(x_\mathrm{I}) \to 1$ and smaller D_2 are allowed because the rate-limiting step is hitting the target from the inner region. In both limits, however, the overall

enhancement effect with respect to a standard random walk becomes negligible. Away from these limits the gain of the optimal heterogeneity is larger for higher dimensions and can be remarkably large for intermediate interface positions [see the inset of Figs. 5(e) and 5(f)] and increases with decreasing target size.

In a biological context, the present setting is relevant for signaling proteins searching for their target in the nucleus when the proteins are initially uniformly distributed throughout the cell cytoplasm. Recent experiments revealed a significant heterogeneity in the spatial dependence of the protein diffusion coefficient across the cell, with a faster diffusivity near the nucleus [60,61]. Such a spatial heterogeneity could therefore be beneficial for the cell by accelerating the dynamics of signaling molecules.

VI. MEAN FIRST-PASSAGE TIME IN A RANDOM HETEROGENEOUS SYSTEM FOR FIXED INITIAL POSITION

We now address the MFPT problem when the interface position is random in a given realization and uniformly distributed over the radial domain. Specifically, we are interested in the MFPT of a particle starting at x_0 averaged over the interface position x_{I},

$$\{\mathbf{T}\}(x_0) = \frac{1}{1-x_a}\int_{x_a}^{1}\mathbf{T}(x_0)dx_{\mathrm{I}}. \tag{19}$$

Experimentally, this would correspond to measuring an ensemble of systems with random value of x_{I}. For dimensions $d = 1$, 2, and 3 the MFPT $\{\mathbf{T}\}(x_0)$ has the explicit form

$$_1\{\mathbf{T}\}(x_0) = \frac{R^2}{2\overline{D}}x_0\left\{1 + \frac{1}{\varphi} + \left(1 - \frac{3}{\varphi}\right)x_0\left[\frac{1}{2} + \left(1 - \frac{1}{\varphi}\right)x_0\right] + \frac{(1-\varphi)^2 x_0^3}{4\varphi}\right\}, \tag{20a}$$

$$_2\{\mathbf{T}\}(x_0) = \frac{R^2}{12\overline{D}(1-x_a^2)(1-x_a)}\left\{\left(1 + \frac{1}{\varphi}\right)x_0\left(6\left(1 - \varphi x_a^2\right) - \frac{2x_0^2\left[4 - \varphi\left(1 + 3x_a^2\right)\right]}{3} - \frac{2x_0^4(\varphi-1)}{5}\right)\right.$$

$$- \left(\frac{2}{\varphi} + 1 - x_a\{3 + x_a[3 - x_a(1+2\varphi)]\}\right)\left[2\ln\left(\frac{x_0}{x_a}\right) - x_0^2\right] - \left[6\left(1 - \frac{1}{\varphi}\right)\right.$$

$$\left.\left.- x_a\left(1 + \frac{6 - x_a[8 - \varphi(16\varphi - 17)]}{3\varphi}\right) - x_a^2\left(3 - x_a^2\frac{2 + \varphi\{11 + 2\varphi\}}{\varphi}\right)\right]\right\}, \tag{20b}$$

$$_3\{\mathbf{T}\}(x_0) = \frac{R^2}{8\overline{D}(1-x_a)(1-x_a^3)}\left(\frac{1}{3}\left(\frac{1}{\varphi} - 1\right)x_0\{2[5 - \varphi(1 - 4x_a^3)] - (1-\varphi)x_0^3\}\right.$$

$$+ \frac{x_a^3}{3}\left[2\left(4\varphi - 5\frac{1}{\varphi}\right) + x_a^3\left(\frac{1}{\varphi} + 2\varphi\right)\right] + \left(\frac{2}{x_a} + x_a^2\right)\left\{\frac{3}{\varphi} + 1 - 4x_a\left[1 + x_a^2\left(1 - \frac{3x_a}{4}\right)\right]\right\}\right\}$$

$$- \left(\frac{2}{x_0} + x_0^2\right)\left\{\frac{3}{\varphi} + 1 - 4x_a\left[1 + x_a^2\left(1 - \frac{(3\varphi + 1)x_a}{4}\right)\right]\right\}\right\}$$

$$- 8\left(\frac{1}{\varphi} - 1\right)\left(1 - \varphi x_a^3\right)\ln\left(\frac{x_0}{x_a}\right)\right). \tag{20c}$$

The gain compared to the homogeneous random walk

$$\{\theta(x_0)\} = \frac{\{\mathbf{T}\}(x_0)}{\mathbf{T}(x_0)} \tag{21}$$

is shown in Figs. 6(a)–6(c) and reveals a somewhat less sharp optimal heterogeneity as compared to the global MFPT. The limiting behavior for small and large φ is the same as for the previous cases, but here there is a wider range of φ values producing a comparable gain. We also observe a stronger dependence on the starting position as $\varphi \to \infty$ and a very weak dependence for $\varphi \to 0$, which is yet another consequence of direct trajectories dominating the MFPT. The optimal heterogeneity is obtained from Eq. (9) and reads

$$_1\{\varphi\}^* = \frac{1}{x_0}\left(\frac{3(2 - x_0)[2 - x_0(2 - x_0)]}{4 - 3x_0}\right)^{1/2}, \tag{22a}$$

$$_2\{\varphi\}^* = \left(\frac{2\ln(x_0/x_a) - 3[Q_1(x_0) - Q_1(x_a)]}{2x_a^3\ln(x_0/x_a) + Q_2(x_0,x_a)}\right)^{1/2}, \tag{22b}$$

$$_3\{\varphi\}^* = \left(\frac{24\ln(x_0/x_a) + Q_3(x_0) - Q_3(x_a)}{24x_a^3\ln(x_0/x_a) - Q_4(x_0,x_a)}\right)^{1/2}. \tag{22c}$$

Here we introduced the auxiliary functions

$$Q_1(y) = y\left[3 + y\left(1 - \frac{4y}{3} + \frac{y^3}{5}\right)\right], \tag{23a}$$

$$Q_2(y,z) = y^3\left(\frac{1}{3} - \frac{y^2}{5}\right) - z^2\left[y(3 - y^2)\right.$$

$$\left.- z\left(\frac{8}{3} - y^2\right) - \frac{z^3}{5}\right], \tag{23b}$$

$$Q_3(y) = \frac{18}{y} + y^2[9 - y(10 - y^3)], \tag{23c}$$

$$Q_4(y,z) = y^3[2(1 + y^2z) - y^3] + z^3(2 + y^3)\left(8 - \frac{9z}{y}\right). \tag{23d}$$
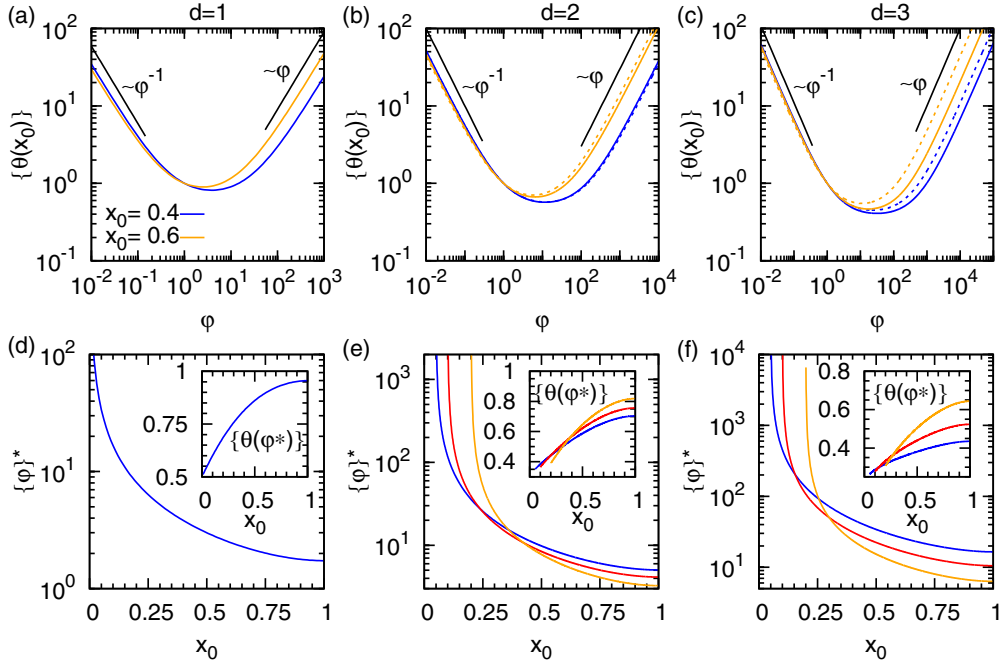
FIG. 6. (Color online) Ratio $\{\theta\} = \{T\}/T(x_0)$ as a function of $\varphi = D_1/D_2$ for different dimensions and $x_0 = 0.4$ (blue) and $x_0 = 0.6$ (orange). The target sizes in (b) and (c) are $x_a = 0.1$ (solid lines) and $x_a = 0.2$ (dashed lines). (d)–(f) Optimal heterogeneity for different dimensions as a function of the starting position x_0. In (e) and (f) the target sizes are $x_a = 0.05$ (blue), $x_a = 0.1$ (red), and $x_a = 0.2$ (orange). The insets in (d)–(f) show $\{\theta\}$ for the optimal heterogeneity $\{\varphi^*\}$.

The results for various dimensions are depicted in Figs. 6(d)–6(f). Accordingly, an optimal heterogeneity always exists. Note that the dependence of $\{\varphi\}^*$ on the target size in $d = 2$ and 3 becomes reversed upon increasing the initial separation to the target. When starting near the target the initial position will on average lie in the inner region in an ensemble of realizations of the interface position. The optimal heterogeneity will thus on average correspond to a very fast diffusion in the inner region. For small x_0 the probability of starting in the inner region $(1 - x_0)/(1 - x_a)$ will be lower for smaller targets and hence $\{\varphi\}^*$ will be larger accordingly. Conversely, if starting farther away from the target x_0 will on average lie in the outer region and the search time will be more strongly influenced by the rate of arriving at the interface in each realization. An optimal heterogeneity will therefore correspond to a smaller asymmetry of diffusivities in the inner and outer regions. More specifically, since the probability of starting in the outer region $(x_0 - x_a)/(1 - x_a)$ will be lower for larger targets, the value of $\{\varphi\}^*$ will accordingly be smaller. The gain of the optimal heterogeneity is shown in the insets of Figs. 6(d)–6(f) and reveals a significant improvement with

respect to the standard random walk in every dimension. The dependence on target size has again a nonmonotonic behavior, which follows from the argument presented above. Hence, even in a system with a random and quenched position of the interface a spatially heterogeneous search process will on average strongly outperform the standard random walk in every dimension.

In a biological context the present setting is important for the experimentally observed quenched spatial disorder revealed by single-particle tracking [61,62,65,74–76]. More generally, the ideas can also be extended to the dynamics in complex disordered systems [77,78] and Sinai-type diffusion [79]. Our results show that quenched spatial heterogeneity can robustly enhance random search processes even in a disordered setting. This robustness could eventually be exploited in search strategies, because it requires less prior knowledge about the location of the target. Note, however, that our model assumes a generic spherical symmetry, such that corrections may be needed to quantitatively describe the above-mentioned biological systems [61,62,65,74–76].

VII. GLOBAL MEAN FIRST-PASSAGE TIME IN A RANDOM SYSTEM

This section completes our study, addressing the global MFPT in a random system

$$\{\overline{T}\} = \frac{1}{1 - x_a} \int_{x_a}^{1} \overline{T} \, dx_I. \tag{24}$$
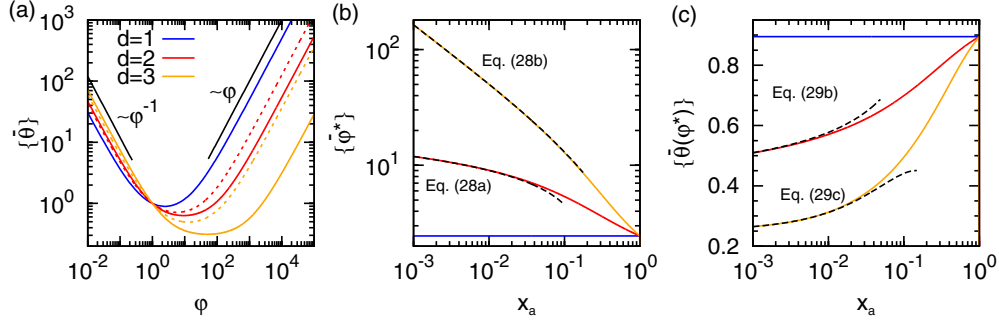
FIG. 7. (Color online) (a) Ratio $\{\bar{\theta}\} = \{\overline{\mathbf{T}}\}/\overline{\mathbf{T}}$ as a function of $\varphi = D_1/D_2$ for different dimensions and target sizes $x_a = 0.1$ (solid lines) and $x_a = 0.01$ (dashed lines). (b) Optimal heterogeneity as a function of the target size. (c) $\{\bar{\theta}\}$ for the optimal strategy as a function of the target size.

As far as a blind spatially heterogeneous search is concerned, this is the most robust setting. It can be shown that the exact results for $\{\overline{\mathbf{T}}\}$ have the form

$$_1\{\overline{\mathbf{T}}\} = \frac{R^2}{60\overline{D}}\left[13 + \varphi + \frac{6}{\varphi}\right], \tag{25a}$$

$$_2\{\overline{\mathbf{T}}\} = \frac{R^2}{2\overline{D}(1-x_a^2)^2(1-x_a)}\left[-\frac{127}{63\varphi} + \frac{293}{630} + \left(\frac{4}{3\varphi} - 3\right)x_a + \frac{1}{30}\left(\frac{40}{\varphi} + 97 - 32\varphi\right)x_a^2\right.$$
$$+ \frac{7}{18}\left(1 - \frac{4}{\varphi}\right)(1+2\varphi)x_a^3 - \frac{1}{6}\left(\frac{2}{\varphi} + 13\right)x_a^4 + \frac{1}{30}\left(\frac{20}{\varphi} + 47 + 8\varphi\right)x_a^5 + \frac{1}{2}x_a^6$$
$$\left. - \frac{1}{240}\left(\frac{20}{\varphi} + 79 + 6\varphi\right)x_a^7 - \frac{2}{3}\left(\frac{2}{\varphi} + 1 + x_a\{-3 + x_a[-3 + x_a(1+2\varphi)]\}\right)\ln(x_a)\right], \tag{25b}$$

$$_3\{\overline{\mathbf{T}}\} = \frac{R^2}{40\overline{D}(1-x_a^3)^2(1-x_a)}\left[\frac{45}{x_a}\left(1 + \frac{3}{\varphi}\right) - \frac{148}{\varphi} - 361 + 5\varphi + 324x_a + 135\left(\frac{1}{\varphi} - 1\right)x_a^2\right.$$
$$+ 3\left(-\frac{45}{\varphi} + 83 + 70\varphi\right)x_a^3 - 81(1+3\varphi)x_a^4 - 27\left(\frac{1}{\varphi} + 7\right)x_a^5 + 3\left(\frac{15}{\varphi} + 47 + 10\varphi\right)x_a^6$$
$$\left. + 36x_a^8 - \left(\frac{5}{\varphi} + 29 + 2\varphi\right)x_a^9 + 18\left(1 - \frac{1}{\varphi}\right)\left(x_a^3 - \frac{1}{\varphi}\right)\ln(x_a)\right]. \tag{25c}$$

The relative gain

$$\{\bar{\theta}\} = \frac{\{\overline{\mathbf{T}}\}}{\overline{\mathbf{T}}} \tag{26}$$

with respect to the global MFPT for the standard random walk is shown in Fig. 7. The limiting scaling as $\varphi \to 0$ and $\varphi \to \infty$ remains unchanged and the dependence of the overall gain on the target size becomes significant for large φ. The optimal heterogeneity in the different spatial dimensions is obtained in the form

$$_1\{\bar{\varphi}\}^* = \sqrt{6}, \tag{27a}$$

$$_2\{\bar{\varphi}\}^* = \sqrt{5}\left(\frac{-127 - 84\ln(x_a) + x_a[126 + x_a(84 - x_a\{98 + 3x_a[7 - 2x_a(7 - x_a^2)]\})]}{16 - 420x_a^3\ln(x_a) - x_a^2\{336 - x_a[245 + 3x_a^2(28 - 3x_a^2)]\}}\right)^{1/2}, \tag{27b}$$

$$_3\{\bar{\varphi}\}^* = \left(\frac{135/x_a - 148 + x_a^2\{135 - x_a[135 - x_a^2(9 - x_a^3)]\} + 180\ln(x_a)}{5 + x_a^3\{210 - x_a[243 - x_a^2(30 - 2x_a^3)]\} + 180x_a^3\ln(x_a)}\right)^{1/2}. \tag{27c}$$

The results are plotted in Fig. 7(a). It can be shown that the results in the $d = 2$ and $d = 3$ cases converge to the result obtained in the $d = 1$ in the limit $x_a \to 1$. This is expected since the system effectively becomes one dimensional when the ratio of the

annulus thickness to the curvature approaches zero. In the other limit $x_a \to 0$ we find the diverging optimal heterogeneity [see Fig. 7(b)]

$$_2\{\overline{\varphi}\}^* \simeq \frac{\sqrt{5[-127 - 84\ln(x_a)]}}{4} \tag{28a}$$

in $d = 2$ and

$$_3\{\overline{\varphi}\}^* \simeq \sqrt{\frac{27}{x_a} - \frac{148}{5}} \tag{28b}$$

in $d = 3$. The gain of the optimal heterogeneity is shown in Fig. 7(c). In $d = 1$ the optimal gain is

$$_1\{\overline{\theta}\}^* = (13 + 2\sqrt{6})/29 \simeq 0.894\,95 \tag{29a}$$

and the expected convergence to this result in higher d as $x_a \to 1$ is depicted in Fig. 7(c). In the corresponding limit $x_a \to 0$ the optimal gain in $d = 2$ behaves as

$$_2\{\overline{\theta}\}^* \simeq \left[\frac{2032}{\sqrt{5[-127 - 84\ln(x_a)]}} - 293/5 + \ln(x_a)\left(\frac{1344}{\sqrt{5[-127 - 84\ln(x_a)]}} + 84 \right) \right] \Big/ 63[3 + 4\ln(x_a)], \tag{29b}$$

ultimately converging logarithmically to $1/3$. Conversely, in $d = 3$ the gain converges to $1/4$ much more rapidly,

$$_3\{\overline{\theta}\}^* \simeq \frac{1}{4} + \sqrt{\frac{x_a}{12}} - \left(\frac{47}{36} + \ln(x_a) \right) x_a. \tag{29c}$$

We therefore find that for vanishingly small targets an optimal heterogeneous search in a random system configuration with uniformly distributed starting position is remarkably 3 and 4 times faster, respectively, in two and three dimensions. We should stress here that this gain is achieved under the constraint of a conserved $\overline{D}$, which means that we do not introduce any additional resources. This is in striking contrast to the optimization of active-passive intermittent strategies, where the ballistic excursions based on active motion are by definition more expensive [5,8,51–57]. If we were to relax the constraint on the conserved $\overline{D}$, the gain could in principle become arbitrarily large.

VIII. DISCUSSION AND CONCLUDING REMARKS

We analyzed the kinetics of a Brownian search in quenched heterogeneous media. Analyzing a minimal model system capturing the fundamental physical aspects of the problem, we obtained exact analytical results for the MFPT of a particle to find the target in various settings. We showed that the MFPT for a Brownian search, both homogeneous and spatially heterogeneous, is dominated by direct trajectories and the results for the MFPT are insensitive to possible excursions to the outer region of our model system away from the target. Under the constraint of conserved average dynamics, we proved the existence of an optimal heterogeneity, which minimizes the MFPT.

We demonstrated and explained how a blind diffusive searcher in a spatially heterogeneous environment can significantly outperform the homogeneous random walk when the motion is faster near the target. This gain, which depends on the size of the target, is significant and persists upon averaging

over the starting position, interface position, or even both. The enhancement is hence very robust. In contrast to conventional search strategies (intermittent or Lévy-stable motion), which have the highest gain in lower dimensions, the heterogeneous search performs best in higher dimensions. Because the MFPT is dominated by direct trajectories and the heterogeneity does not affect the compactness of exploring the surrounding space, but instead acts by enhancing or retarding the local dynamics, it performs better for noncompact exploration.

According to recent single-particle-tracking experiments in living cells, the diffusivity of smaller proteins is faster close to the nucleus and slower in the cell periphery [60,61]. In addition, even in the presence of quenched spatially disordered heterogeneity, which is often observed in particle-tracking experiments inside cells [61,62,74–76], the target search kinetics can be enhanced as well, even if the process starts from a spatially uniform initial distribution of the searching molecules. Inside cells signaling proteins are found at extremely low concentrations, down to, for instance, a dozen of λ-repressor molecules searching for a single target in an *E. coli* cell, whose volume is about 1 μm^3. The search kinetics is thus central and rate limiting for signaling dynamics. Hence, heterogeneous search processes are important and relevant phenomena at the few-molecule level.

At this point a few additional remarks are in order. The additivity in Eq. (6) only holds for the MFPT and not for higher moments. Based on our present arguments, the additivity principle in Eq. (6) should hold for an arbitrary number of segments, but a formal proof is part of our current investigation. If this is indeed the case, an optimal heterogeneity function can be formally constructed for any situation by first taking the appropriate limits of small segments and afterward optimizing

using variational methods. The underlying physical principle, however, will remain unchanged. This will allow the study of more realistic heterogeneity profiles such as those observed experimentally in living cells [60–62,74–76].

In the present context the optimization of diffusion heterogeneity cannot be perceived as a search strategy in the traditional sense [5,8,18–21,23]. A searcher would somehow have to know the position of the target in order to optimize his motion pattern according to an optimal heterogeneity. Conversely, in a cell the position of the target is given and so are the cytoplasm and nucleus properties giving rise to a spatially varying diffusivity. However, it could be part of an evolutionary optimization to improve the search efficiency of biomolecules in cell regulatory processes.

The present results can be extended and generalized in numerous ways, the immediate extension being the study of the full distribution of first-passage times. Furthermore, within the context of a traditional search strategy, our findings cannot be directly used to assess the efficiency of a heterogeneous search with a general off-center target position as in [50]. The optimization of the target-position-averaged MFPT with respect to the ratio φ of diffusivities continues to be investigated. Given the present results, we can speculate, however, that an enhancement might indeed be possible in terms of an optimal heterogeneity at least for target positions not too close to the external boundary. One can therefore imagine that heterogeneous search strategies are also beneficial for computer search or stochastic minimization algorithms. The ideas can be generalized to diffusion processes in more complex disordered systems [77–79] and even anomalous diffusion processes of continuous-time random-walk type [80]. Namely, in a finite system the heavy-tailed waiting-time density between individual jumps in a subdiffusive continuous-time random walk is expected to be exponentially tempered, exhibiting subdiffusion over a transient but long-time scale, which would ultimately terminate with a normal diffusion regime. In such a system the MFPT to the target will be finite and it would be interesting to investigate how, if at all, the existence and properties of an *optimal heterogeneity* change in a heterogeneous system with transiently subdiffusive dynamics. The most obvious extension of the present results, however, is in the direction of a heterogeneous intermittent search. Clearly, a combination of both could lead to a highly superior search dynamics.

APPENDIX: COMPUTER SIMULATION RESULTS

Computer simulations were performed according to the scheme of transition probabilities outlined in Sec. II. We simulated 10^5 trajectories for each set of x_a, x_i, and/or x_0. The simulations correspond to a discrete random walk in between spherical shells with an absorbing boundary at $x = x_a$ and a reflecting one at $x = 1$ recording the number of steps within each region $n_{1,2}$ as well as the total number of steps n to obtain the process time according to

$$t = \frac{\Delta R^2}{2D_1}(n_1 - n_2 + n) + \frac{\Delta R^2}{2D_2}(n_2 - n_1 + n). \quad \text{(A1)}$$

Note that n also counts the number of steps in the interfacial shells. The results for various cases are plotted below. We find remarkably good agreement between our analytical results and the simulation results. The MFPT as a function of the interface position is shown in Fig. 8. Intuitively, the MFPT depends strongly on the starting and interface positions and can exhibit zero, one, or two local minima as a function of x_I. Hence, it is possible for a given φ that two distinct interface positions lead to the same MFPT. It should be noted that an equal φ does not correspond to equal D_1 and D_2; only their ratio is fixed. A degeneracy of the MFPT depending on the interface position is thus not surprising. The simulation results for the global MFPT are shown in Fig. 9 and compared to the analytical predictions of Sec. V. In the case of the global MFPT as well, zero, one, or two minima are observed depending on φ. Here we observe significant differences in the features of the global MFTP at equal φ in different dimensions. This is due to the fact that the statistical weight of various starting positions is different in different dimensions and more distant starting configurations have a higher weight in higher dimensions. The simulation results for the interface-position-averaged MFPT in a random
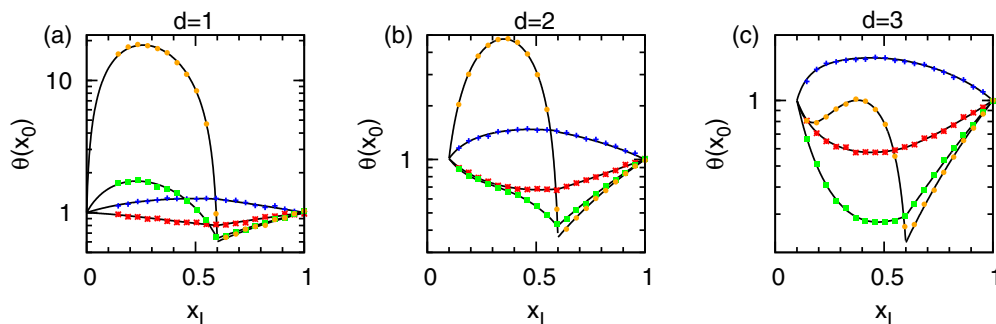

FIG. 8. (Color online) Ratio $\theta = \mathbf{T}(x_0)/\mathbf{T}^0(x_0)$ as a function of x_I for $x_0 = 0.6$ and $x_a = 0.1$ in different dimensions. The colors depict results for various heterogeneities: $\varphi = 0.6$ (blue), 2 (red), 10 (green), and 150 (orange). The symbols are results of simulations and the solid lines correspond to the analytical results in Eqs. (12).
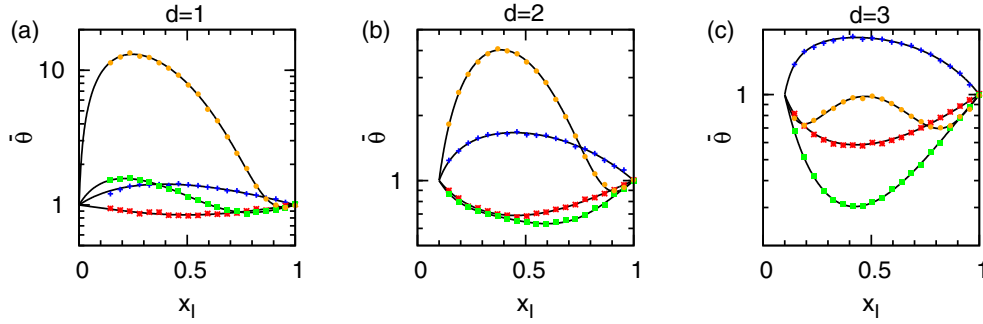
FIG. 9. (Color online) Ratio $\bar{\theta} = \overline{\mathbf{T}}/\overline{\mathbf{T}}^0$ as a function of x_I for $x_a = 0.1$ in different dimensions. The colors depict results for various heterogeneities: $\varphi = 0.5$ (blue), 2 (red), 10 (green), and 120 (orange). The symbols are results of simulations and the solid lines correspond to the analytical results in Eqs. (25).

system are shown in Fig. 10 and compared to the analytical predictions of Sec. VI. In the case of the MFPT with a random interface position, the disorder-averaged MFPT (Fig. 10) is only weakly dependent on x_0 as long as φ is not too large. Again, very distinct behavior is found for different dimensions at equal φ. In contrast to the global MFPT, this originates solely from the differences in the exploration of space. The results

for the interface-position-averaged global MFPT in a random system are shown in Fig. 11. Here also we find excellent agreement between theory and simulation. We see that the dependence on the target size becomes more prominent in higher dimensions because of the different statistical weight of starting positions at a given distance from x_a and the differences in sampling space.
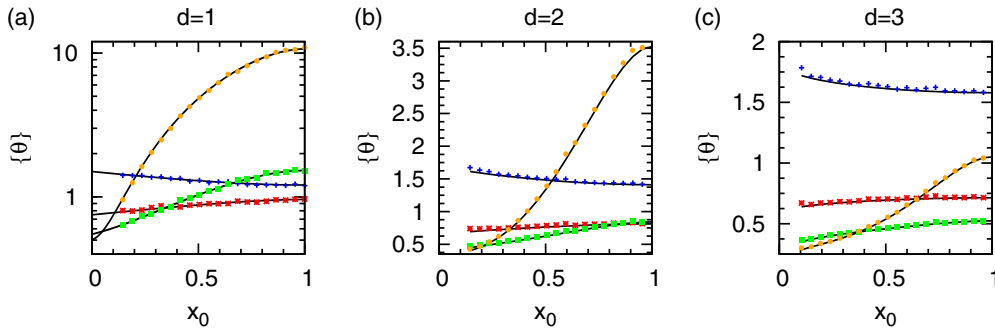

FIG. 10. (Color online) Ratio $\{\theta\} = \{\mathbf{T}\}/\mathbf{T}(x_0)$ as a function of x_0 for $x_a = 0.1$ in different dimensions. The colors depict results for various heterogeneities: $\varphi = 0.5$ (blue), 2 (red), 10 (green), and 120 (orange). The symbols are results of simulations and the solid lines correspond to the analytical results in Eqs. (20).
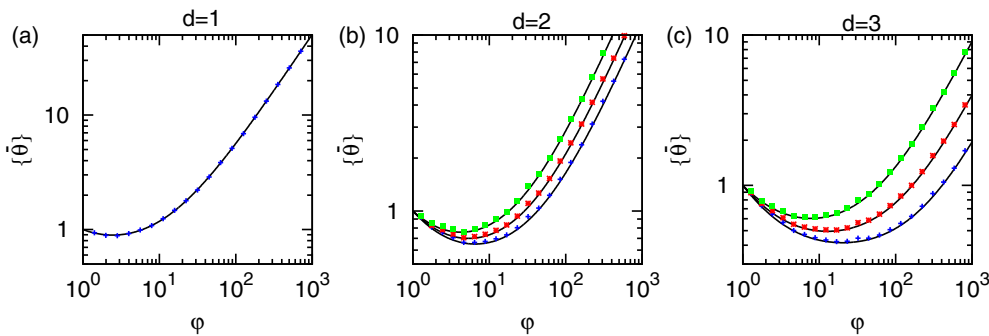

FIG. 11. (Color online) (a) Ratio $\{\bar{\theta}\} = \{\overline{\mathbf{T}}\}/\overline{\mathbf{T}}$ as a function of φ for different dimensions and target sizes. In dimensions (b) 2 and (c) 3 the target sizes correspond to 0.05 (blue), 0.1 (red), and 0.2 (green).

[1] W. J. Bell, *Searching Behaviour* (Chapman and Hall, London, 1991).

[2] H. C. Berg, *Random Walks in Biology* (Princeton University Press, Princeton, 1993).

[3] L. A. Lloyd and R. M. May, Epidemiology: How viruses spread among computers and people, Science **292**, 1316 (2001).

[4] V. Belik, T. Geisel, and D. Brockmann, Natural human mobility patterns and spatial spread of infectious diseases, Phys. Rev. X **1**, 011001 (2011).

[5] O. Bénichou, C. Loverdo, M. Moreau, and R. Voituriez, Intermittent search strategies, Rev. Mod. Phys. **83**, 81 (2011).

[6] A. J. Bray, S. Majumdar, and G. Schehr, Persistence and first-passage properties in nonequilibrium systems, Adv. Phys. **62**, 325 (2013).

[7] S. Condamin, O. Bénichou, V. Tejedor, R. Voituriez, and J. Klafter, First-passage times in complex scale-invariant media, Nature (London) **450**, 77 (2007).

[8] P. C. Bressloff and M. J. Newby, Stochastic models of intracellular transport, Rev. Mod. Phys. **85**, 135 (2013).

[9] S. Condamin, O. Bénichou, and M. Moreau, First-passage times for random walks in bounded domains, Phys. Rev. Lett. **95**, 260601 (2005).

[10] D. Holcman, A. Marchewka, and Z. Schuss, Survival probability of diffusion with trapping in cellular neurobiology, Phys. Rev. E **72**, 031910 (2005).

[11] Z. Schuss, A. Singer, and D. Holcman, The narrow escape problem for diffusion in cellular microdomains, Proc. Natl. Acad. Sci. USA **104**, 16098 (2007).

[12] O. Bénichou, B. Meyer, V. Tejedor, and R. Voituriez, Zero constant formula for first-passage observables in bounded domains, Phys. Rev. Lett. **101**, 130601 (2008).

[13] V. Tejedor, O. Bénichou, and R. Voituriez, Global mean first-passage times of random walks on complex networks, Phys. Rev. E **80**, 065104(R) (2009).

[14] A. Amitai and D. Holcman, Diffusing polymers in confined microdomains and estimation of chromosomal territory sizes from chromosome capture data, Phys. Rev. Lett. **110**, 248105 (2013).

[15] P. C. Bressloff, Stochastic model of intraflagellar transport, Phys. Rev. E **73**, 061916 (2006).

[16] T. G. Mattos, C. Mejía-Monasterio, R. Metzler, and G. Oshanin, First passages in bounded domains: When is the mean first passage time meaningful?, Phys. Rev. E **86**, 031143 (2012).

[17] C. Mejía-Monasterio, G. Oshanin, and G. Schehr, First passages for a search by a swarm of independent random searchers, J. Stat. Mech. (2011) P06022.

[18] D. Holcman and Z. Schuss, Time scale of diffusion in molecular cellular biology, J. Phys. A **47**, 173001 (2014).

[19] M. Sheinman, O. Bénichou, Y. Kafri, and R. Voituriez, Classes of fast and specific search mechanisms for proteins on DNA, Rep. Prog. Phys. **75**, 026601 (2012).

[20] M. Bauer and R. Metzler, In vivo facilitated diffusion model, PLoS ONE **8**, e53956 (2013).

[21] O. Pulkkinen and R. Metzler, Distance matters: The impact of gene proximity in bacterial gene regulation, Phys. Rev. Lett. **110**, 198101 (2013).

[22] B. van den Broek, M. A. Lomholt, S.-M. J. Kalisch, R. Metzler, and G. J. L. Wuite, How DNA coiling enhances target localization by proteins, Proc. Natl. Acad. Sci. USA **105**, 15738 (2008).

[23] M. A. Lomholt, B. van den Broek, S.-M. J. Kalisch, G. J. L. Wuite, and R. Metzler, Facilitated diffusion with DNA coiling, Proc. Natl. Acad. Sci. USA **106**, 8204 (2009).

[24] O. Bénichou, C. Chevalier, B. Meyer, and R. Voituriez, Facilitated diffusion of proteins on chromatin, Phys. Rev. Lett. **106**, 038102 (2011).

[25] O. Bénichou, Y. Kafri, M. Sheinman, and R. Voituriez, Searching fast for a target on DNA without falling to traps, Phys. Rev. Lett. **103**, 138102 (2009).

[26] I. Pavlyukevich, Lévy flights, non-local search and simulated annealing, J. Comput. Phys. **226**, 1830 (2007).

[27] S. Redner, *A Guide to First Passage Processes* (Cambridge University Press, New York, 2001).

[28] *First-Passage Phenomena and Their Applications*, edited by R. Metzler, G. Oshanin, and S. Redner (World Scientific, Singapore, 2014).

[29] D. Brockmann and T. Geisel, Lévy flights in inhomogeneous media, Phys. Rev. Lett. **90**, 170601 (2003).

[30] D. Brockmann and T. Geisel, Particle dispersion on rapidly folding random heteropolymers, Phys. Rev. Lett. **91**, 048303 (2003).

[31] M. A. Lomholt, T. Ambjörnsson, and R. Metzler, Optimal target search on a fast-folding polymer chain with volume exchange, Phys. Rev. Lett. **95**, 260603 (2005).

[32] T. Koren, M. A. Lomholt, A. V. Chechkin, J. Klafter, and R. Metzler, Leapover lengths and first passage time statistics for Lévy flights, Phys. Rev. Lett. **99**, 160602 (2007).

[33] V. V. Palyulin, A. V. Chechkin, and R. Metzler, Lévy flights do not always optimize random blind search for sparse targets, Proc. Natl. Acad. Sci. USA **111**, 2931 (2014).

[34] L. Kusmierz, S. N. Majumdar, S. Sabhapandit, and G. Schehr, First order transition for the optimal search time of Lévy flights with resetting, Phys. Rev. Lett. **113**, 220602 (2014).

[35] G. Zumofen and J. Klafter, Scale-invariant motion in intermittent chaotic systems, Phys. Rev. E **47**, 851 (1993).

[36] G. Zumofen and J. Klafter, Power spectra and random walks in intermittent chaotic systems, Physica D **69**, 436 (1993).

[37] T. Geisel, J. Nierwetberg, and A. Zacherl, Accelerated diffusion in Josephson junctions and related chaotic systems, Phys. Rev. Lett. **54**, 616 (1985).

[38] J. Klafter, A. Blumen, and M. F. Shlesinger, Stochastic pathway to anomalous diffusion, Phys. Rev. A **35**, 3081 (1987).

[39] J. Klafter, M. F. Shlesinger, and G. Zumofen, Beyond Brownian motion, Phys. Today **49**, 33 (1996).

[40] A. Godec and R. Metzler, Finite-time effects and ultraweak ergodicity breaking in superdiffusive dynamics, Phys. Rev. Lett. **110**, 020603 (2013).

[41] A. Godec and R. Metzler, Linear response, fluctuation-dissipation, and finite-system-size effects in superdiffusion, Phys. Rev. E **88**, 012116 (2013).

[42] D. Froemberg and E. Barkai, Time-averaged Einstein relation and fluctuating diffusivities for the Lévy walk, Phys. Rev. E **87**, 030104(R) (2013).

[43] D. Froemberg and E. Barkai, Random time averaged diffusivities for Lévy walks, Eur. Phys. J. B **86**, 331 (2013).

[44] M. Niemann, H. Kantz, and E. Barkai, Fluctuations of $1/f$ noise and the low-frequency cutoff paradox, Phys. Rev. Lett. **110**, 140603 (2013).

[45] A. Rebenshtok, S. Denisov, P. Hänggi, and E. Barkai, Infinite densities for Lévy walks, Phys. Rev. E **90**, 062135 (2014).

[46] V. Zaburdaev, S. Denisov, and J. Klafter, Lévy walks, Rev. Mod. Phys. (to be published).

[47] C. A. Brackley, M. E. Cates, and D. Marenduzzo, Facilitated diffusion on mobile DNA: Configurational traps and sequence heterogeneity, Phys. Rev. Lett. **109**, 168103 (2012).

[48] C. A. Brackley, M. E. Cates, and D. Marenduzzo, Intracellular facilitated diffusion: Searchers, crowders, and blockers, Phys. Rev. Lett. **111**, 108101 (2013).

[49] O. Bénichou, D. Grebenkov, P. Levitz, C. Loverdo, and R. Voituriez, Optimal reaction time for surface-mediated diffusion, Phys. Rev. Lett. **105**, 150606 (2010).

[50] T. Calandre, O. Bénichou, and R. Voituriez, Accelerating search kinetics by following boundaries, Phys. Rev. Lett. **112**, 230601 (2014).

[51] M. A. Lomholt, T. Koren, and R. Metzler, and J. Klafter, Lévy strategies in intermittent search processes are advantageous, Proc. Natl. Acad. Sci. USA **105**, 11055 (2008).

[52] G. Oshanin, H. S. Wio, K. Lindenberg, and S. F. Burlatsky, Intermittent random walks for an optimal search strategy: one-dimensional case, J. Phys.: Condens. Matter **19**, 065142 (2007).

[53] G. Oshanin, K. Lindenberg, H. S. Wio, and S. F. Burlatsky, Efficient search by optimized intermittent random walks, J. Phys. A **42**, 434008 (2009).

[54] C. Loverdo, O. Bénichou, M. Moreau, and R. Voituriez, Enhanced reaction kinetics in biological cells, Nat. Phys. **4**, 134 (2008).

[55] C. Loverdo, O. Bénichou, M. Moreau, and R. Voituriez, Robustness of optimal intermittent search strategies in one, two, and three dimensions, Phys. Rev. E **80**, 031146 (2009).

[56] P. C. Bressloff and J. M. Newby, Quasi-steady-state analysis of two-dimensional random intermittent search processes, Phys. Rev. E **83**, 061139 (2011).

[57] P. C. Bressloff and J. M. Newby, Filling of a poisson trap by a population of random intermittent searchers, Phys. Rev. E **85**, 031909 (2012).

[58] O. Bénichou and R. Voituriez, From first-passage times of random walks in confinement to geometry-controlled kinetics, Phys. Rep. **539**, 225 (2014).

[59] J. Masoliver, K. Lindenberg, and B. J. West, First-passage times from non-Markovian processes: Correlated impacts on bound processes, Phys. Rev. A **34**, 2351 (1986).

[60] T. Kühn, T. O. Ihalainen, J. Hyväluoma, N. Dross, S. F. Willman, J. Langowski, M. Vihinen-Ranta, and J. Timonen, Protein diffusion in mammalian cell cytoplasm, PLoS ONE **6**, e22962 (2011).

[61] B. P. English, V. Hauryliuk, A. Sanamrad, S. Tankov, N. H. Dekker, and J. Elf, Single-molecule investigations of the stringent response machinery in living bacterial cells, Proc. Natl. Acad. Sci. USA **108**, E365 (2011).

[62] P. J. Cutler, M. D. Malik, S. Liu, J. M. Byars, D. S. Lidke, and K. A. Lidke, Multi-color quantum dot tracking using a high-speed hyperspectral line-scanning microscope, PLoS ONE **8**, e64320 (2013).

[63] A. G. Cherstvy, A. V. Chechkin, and R. Metzler, Particle invasion, survival, and non-ergodicity in 2D diffusion processes with space-dependent diffusivity, Soft Matter **10**, 1591 (2014).

[64] A. G. Cherstvy, A. V. Chechkin, and R. Metzler, Anomalous diffusion and ergodicity breaking in heterogeneous diffusion processes, New J. Phys. **15**, 083039 (2013).

[65] P. Massignan, C. Manzo, J. A. Torreno-Pina, M. F. García-Parako, M. Lewenstein, and G. L. Lapeyre, Jr., Nonergodic subdiffusion from Brownian motion in an inhomogeneous medium, Phys. Rev. Lett. **112**, 150603 (2014).

[66] X. Zhang, J. Hansing, R. R. Netz, and J. E. DeRouchey, Particle transport through hydrogels Is charge asymmetric, Biophys. J. **108**, 530 (2015); A. Godec, M. Bauer, and R. Metzler, Collective dynamics effect transient subdiffusion of inert tracers in flexible gel networks, New J. Phys. **16**, 092002 (2014).

[67] P. Gouze, Y. Melean, T. Le Borgne, M. Dentz, and J. Carrera, Non-Fickian dispersion in porous media explained by heterogeneous microscale matrix diffusion, Water Resour. Res. **44**, W11416 (2008); T. Ukmar, M. Gaberšček, F. Merzel, and A. Godec, Modus operandi of controlled release from mesoporous matrices: A theoretical perspective, Phys. Chem. Chem. Phys. **13**, 15311 (2011).

[68] Y. L. Klimontovich, Ito, stratonovich and kinetic forms of stochastic equations, Physica A **163**, 515 (1990); Alternative description of stochastic processes in nonlinear systems. Kinetic form of master and Fokker-Planck equations, **182**, 121 (1992); Nonlinear Brownian motion, Phys. Usp. **37**, 737 (1994); P. Hänggi and H. Thomas, Stochastic processes: Time- evolution, symmetries and linear response, Phys. Rep. **88**, 207 (1982); J. Dunkel and P. Hänggi, Theory of relativistic Brownian motion: The (1+3)-dimensional case, Phys. Rev. E **72**, 036106 (2005).

[69] M. Tokuyama and I. Oppenheim, On the theory of concentrated hard-sphere suspensions, Physica A **216**, 85 (1995).

[70] More precisely, the spatially heterogeneous dissipation has a purely fluctuational origin and does not reflect heterogeneities in the static free volume accessible to the proteins and would hence give rise to a spatially uniform steady-state profile in the absence of the absorbing target.

[71] A. W. C. Lau and T. C. Lubensky, State-dependent diffusion: Thermodynamic consistency and its path integral formulation, Phys. Rev. E **76**, 011123 (2007).

[72] T. Ando and J. Skolnick, Crowding and hydrodynamic interactions likely dominate in vivo macromolecular motion, Proc. Natl. Acad. Sci. USA **107**, 18457 (2010).

[73] H. W. McKenzie, M. A. Lewis, and E. H. Merril, First passage time analysis of animal movement and insights into the functional response, Bull. Math. Biol. **71**, 107 (2009).

[74] A. Sergé, N. Bertaux, H. Rigenault, and D. Marguet, Dynamic multiple-target tracing to probe spatiotemporal cartography of cell membranes, Nat. Methods **5**, 687 (2008).

[75] G. Giannone, E. Hosy, J.-B. Sibarita, D. Choquet, and L. Cognet, in *Nanoimaging, Methods in Molecular Biology*, edited by A. A. Sousa and M. J. Kruhlak (Humana, New York, 2013), Vol. 950, pp. 95–110.

[76] J. B. Masson, P. Dionne, C. Salvatico, M. Renner, C. Specht, A. Triller, and M. Dahan, Mapping the energy and diffusion landscapes of membrane proteins at the cell surface using high-density single-molecule imaging and Bayesian inference: Application to the multiscale dynamics of glycine receptors in the neuronal membrane, Biophys. J. **106**, 74 (2014).

[77] M. Khoury, A. M. Lacasta, J. M. Sancho, and K. Lindenberg, Weak disorder: Anomalous transport and diffusion are normal yet again, Phys. Rev. Lett. **106**, 090602 (2011); M. S. Simon, J. M. Sancho, and K. Lindenberg, Transport and diffusion of overdamped Brownian particles in random potentials, Phys. Rev. E **88**, 062105 (2013).

[78] M. A. Lomholt, L. Lizana, R. Metzler, and T. Ambjörnsson, Microscopic origin of the logarithmic time evolution of aging processes in complex systems, Phys. Rev. Lett. **110**, 208301 (2013); L. P. Sanders, M. A. Lomholt, L. Lizana, K. Fogelmark, R. Metzler, and T. Ambjörnsson, Severe slowing-down and universality of the dynamics in disordered interacting many-body systems: Ageing and ultraslow diffusion, New J. Phys. **16**, 113050 (2014).

[79] Ya. G. Sinai, The limiting behavior of a one-dimensional random walk in a random medium, Theory Probab. Appl. **27**, 256 (1982); J.-P. Bouchaud, A. Comtet, A. Georges, and P. Le Doussal, Classical diffusion of a particle in a one-dimensional random force field, Ann. Phys. (NY) **201**, 285 (1990); A. Comtet and D. S. Dean, Exact results on Sinai's diffusion, J. Phys. A **31**, 8595 (1998); D. S. Fisher, P. Le Doussal, and C. Monthus, Nonequilibrium dynamics of random field Ising spin chains:

Exact results via real space renormalization group, Phys. Rev. E **64**, 066107 (2001); P. Le Doussal, C. Monthus, and D. S. Fisher, Random walkers in one-dimensional random environments: Exact renormalization group analysis, *ibid.* **59**, 4795 (1999); D. Boyer, D. S. Dean, C. Mejia-Monasterio, and G. Oshanin, Optimal estimates of the diffusion coefficient of a single Brownian trajectory, *ibid.* **85**, 031136 (2012); G. Oshanin, A. Rosso, and G. Schehr, Anomalous fluctuations of currents in Sinai-type random chains with strongly correlated disorder, Phys. Rev. Lett. **110**, 100602 (2013); A. Godec, A. V. Chechkin, E. Barkai, H. Kantz, and R. Metzler, Localisation and universal fluctuations in ultraslow diffusion processes, J. Phys. A **47**, 492002 (2014); H. Krüsemann, A. Godec, and R. Metzler, First-passage statistics for aging diffusion in systems with annealed and quenched disorder, Phys. Rev. E **89**, 040101(R) (2014); D. S. Dean, S. Gupta, G. Oshanin, A. Rosso, and G. Schehr, Diffusion in periodic, correlated random forcing landscapes, J. Phys. A **47**, 372001 (2014).

[80] J. H. P. Schulz, E. Barkai, and R. Metzler, Ageing effects in single particle trajectory averages, Phys. Rev. Lett. **110**, 020602 (2013); Aging renewal theory and application to random walks, Phys. Rev. X **4**, 011028 (2014).